Soil minerals mediate climatic control of soil C cycling on annual to centennial timescales

Jeffrey Beem-Miller[1], Craig Rasmussen[2], Alison M. Hoyt[1,3], Marion Schrumpf[1], Georg Guggenberger[4], & Susan Trumbore[1]

[1] Department of Biogeochemical Processes, Max Planck Institute for Biogeochemistry, Jena, Germany

[2] Department of Environmental Science, The University of Arizona, Tucson, AZ, USA

[3] Department of Earth System Science, Stanford University, Stanford, CA, USA

[4] Institute of Soil Science, Leibniz University Hannover, Hannover, Germany

Correspondence to: Jeffrey Beem-Miller (jbeem@bgc-jena.mpg.de)

Abstract. Climate and parent material both affect soil C persistence, yet the relative importance of climatic versus mineralogical controls on soil C dynamics remains unclear. To test this, we collected soil samples in 2001, 2009, and 2019 along a combined gradient of parent material (andesite, basalt, granite) and climate (mean annual temperature (MAT): 6.5 °C "cold", 8.6 °C "cool", 12.0 °C "warm"). We measured the radiocarbon of heterotrophically respired CO_2 ($\Delta^{14}C_{respired}$) and bulk soil C ($\Delta^{14}C_{bulk}$) as proxies for transient and persistent soil C, and characterized mineral assemblages using selective dissolution. Using linear regression, we observed that MAT was not a significant predictor of either $\Delta^{14}C_{bulk}$ or $\Delta^{14}C_{respired}$, yet climate was highly significant as a categorical variable. Climate explained more variance in $\Delta^{14}C_{bulk}$ and $\Delta^{14}C_{respired}$ over 0–0.1 m, but parent material explained more from 0.1–0.3 m. Cool site soil C was more persistent (lower $\Delta^{14}C_{bulk}$) than cold or warm climate sites, and also more persistent on andesitic soils, followed by basaltic and then granitic soils. Poorly crystalline metal oxides (PCMs) (but not crystalline metal oxides) were significantly ($p < 0.1$) correlated with $\Delta^{14}C_{bulk}$, $\Delta^{14}C_{respired}$, and $\Delta^{14}C_{respired}$ - $\Delta^{14}C_{bulk}$, indicating their importance for soil C cycling on both short and long timescales. The change in $\Delta^{14}C_{respired}$ observed over the study period was linearly related to MAT for the granite soils with the lowest PCM content, but not in the andesitic and basaltic soils with higher PCM content. This link between PCM abundance and the decoupling of MAT and soil C cycling rates suggests PCMs may attenuate the temperature sensitivity of decomposition.

1 Introduction

Understanding the response of soil carbon stocks to current and future changes in climate requires insight into the environmental factors governing soil carbon dynamics. Climate, and in particular temperature, has been found to be the most important variable for explaining the age of soil carbon in topsoil at local to global scales (Frank et al., 2012; Mathieu et al., 2015; Shi et al., 2020). Yet our current understanding of soil organic matter decomposition underscores the importance of mechanisms that can affect the temperature sensitivity of decomposition, such as the interaction between soil organic matter and minerals (Davidson et al., 2000; Rasmussen et al., 2005; Davidson and Janssens, 2006; Lehmann and Kleber, 2015). The

effect of mineral-organic associations on the temperature sensitivity of soil organic matter has been addressed in several modeling studies (Tang and Riley, 2014; Abramoff et al., 2019; Woolf and Lehmann, 2019; Ahrens et al., 2020). These models typically invoke Michaelis Menten kinetics in addition to an Arrhenius-type temperature response in order to account for energy and substrate limitations on decomposition rates of soil organic matter found in association with minerals (Tang and Riley, 2019; Ahrens et al., 2020). In situ studies comparing the role of soil mineral assemblages and temperature in explaining soil C dynamics over time are scarce, yet are critical for testing model-based findings. We designed the current study to quantify the relative importance of climatic versus mineralogical mechanisms of soil organic C persistence across a combined gradient of mean annual temperature (MAT) and parent material in order to provide insight into the relevant time scales associated with these key soil forming factors.

The relevance of soil minerals for mediating soil organic matter protection has been found to be a function of the specific minerals present, rather than the amount of clay or total mineral surface area (Kramer and Chadwick, 2018; Rasmussen et al., 2018a). Soil mineral assemblages are dynamic, developing over time as primary minerals inherited from parent material weather to form reactive, poorly crystalline secondary minerals, which in turn eventually weather or ripen into increasing stable crystalline species (Mikutta et al., 2010; Slessarev et al., 2022). Soils enriched in poorly crystalline metal oxides (PCMs), such as Al and Fe oxyhydroxides, are known to be of particular importance for the accumulation and persistence of soil C (Torn et al., 1997; Masiello et al., 2004). The abundance of these minerals in soils is directly related to parent material, but is also a function of primary mineral weathering rates (Slessarev et al., 2022). Due to the strong effect of climate on weathering, different soil mineral assemblages can form from the same parent material under different climatic regimes (Kramer and Chadwick, 2016; Rasmussen et al., 2018b). Conversely, similar mineral assemblages can be found among soils developed on different parent materials given adequate time for weathering and similar vegetation and climate (Graham and O'Geen, 2010). These complex interactions demonstrate that climatic and mineralogical controls on soil C cycling are not independent, but interact over the centennial to millennial time scales of soil development.

The strength and sorptive capacity of soil minerals is dependent on ligand exchange, which is a function of not only surface area and charge, but more specifically the density of accessible hydroxyl groups (Kaiser and Guggenberger, 2003; Kleber et al., 2015; Rasmussen et al., 2018a). Poorly crystalline metal oxides are particularly enriched in hydroxyl groups, and batch sorption/desorption experiments have shown that the mineral-organic interactions between pedogenic metal oxide-rich clays are stronger than those with siloxane-rich phyllosilicate clays (Kahle et al., 2004). Furthermore, the reactive properties of pedogenic metal oxides can also facilitate lower strength interactions with soil organic matter through multivalent cation bridging (Kleber et al., 2007). This high reactivity of poorly crystalline Fe oxides is also implicated in the observations that poorly crystalline Fe is correlated with aggregate stability but crystalline Fe oxide content is not (Duiker et al., 2003). Consequently, Rasmussen et al. (2018b) observed that oxalate extractable iron, as an extractant for PCM, was the best predictor both soil C concentration and $\Delta^{14}C_{bulk}$. However, the relevance of mineral-organic associations with specific

mineral phases such as PCM or crystalline metal oxides (CRM) for specific timescales of soil C turnover is poorly studied (Heckman et al., 2018).

Radiocarbon (^{14}C) is a useful tracer for soil C dynamics over annual to millennial time scales (Trumbore, 2000). The use of ^{14}C to measure timescales of soil carbon decomposition is reliant on our knowledge of the $^{12}C/^{14}C$ ratio of atmospheric CO_2. Once CO_2 is fixed into organic matter via photosynthesis this ratio starts to shift, as ^{14}C is preferentially lost due to radioactive decay. Changes in the $^{12}C/^{14}C$ ratio due to radioactive decay are detectable at timescales of hundreds to thousands of years. However, we can detect changes in ^{14}C with nearly annual resolution for the so-called "bomb-C" period, which began with the atmospheric testing of nuclear weapons in the mid-20th century (Trumbore, 2000). This pulse of "bomb-C" led to a doubling of atmospheric ^{14}C concentration prior to the ban on above-ground nuclear tests in 1963 (Hua et al., 2021). The level of ^{14}C in the atmosphere returned to pre-bomb levels around 2020, thus archived samples now represent the best opportunity to construct a high-resolution time series of the bomb-C pulse as it moves through different soil organic matter pools (Trumbore, 2009).

Soil is an open system, and this has important implications for the interpretation of radiocarbon measurements of soil C. For most soils, the majority of carbon that enters the soil leaves relatively quickly, with only a small fraction persisting (Sierra et al., 2018; Crow and Sierra, 2022). The signal from these persistent pools typically dominate measurements of $\Delta^{14}C_{bulk}$, while the signal from more transient pools makes up the majority of C leaving the soil via heterotrophic respiration, captured through measurements of $\Delta^{14}C_{respired}$ (Trumbore, 2000). Here we define "transient" for C cycling on annual to decadal timescales, while we use "persistent" to refer to C cycling on centennial to millennial timescales. A diagnostic feature of $\Delta^{14}C_{bulk}$ and $\Delta^{14}C_{respired}$ is that when these two metrics are the same, this indicates all of the C in the soil has an equal probability of being decomposed by microbes and that the system is homogenous (Sierra et al., 2017). However, when $\Delta^{14}C_{bulk}$ and $\Delta^{14}C_{respired}$ are substantially different, this indicates the presence of both labile and persistent pools of soil C (Ewing et al., 2006; Hopkins et al., 2012).

We turned to the western slope of the Sierra Nevada Mountains, USA to compare and contrast the effects of climate and mineral assemblage on soil C dynamics. Drawing on earlier studies in this region (Jenny et al., 1949; Trumbore et al., 1996, p.199; Dahlgren et al., 1997; Rasmussen, 2004), we selected soils similar in age and vegetation along a combined gradient of parent material (granite, andesite, basalt) and MAT (6.5 °C, 8.6 °C, 12.0 °C). The climate gradient also represents a weathering gradient, with poorly developed soils at the cold climate sites, intermediately developed soils at the cool climate sites, and highly weathered soils at the warm climate sites (Harradine and Jenny, 1958; Rasmussen et al., 2010a). Previous work at these sites (Rasmussen, 2004; Rasmussen et al., 2018b) and nearby locations (Trumbore et al., 1996; Dahlgren et al., 1997; Castanha et al., 2008; Koarashi et al., 2012) confirmed strong differences in mineral assemblages along both the parent material and climate gradients, making these sites an ideal setting for probing the relative influence of climatic and mineralogical factors (and their interactions), on soil C dynamics.

We were able to construct a time series of both $\Delta^{14}C_{bulk}$ and $\Delta^{14}C_{respired}$ at these sites by combining data from samples newly collected in 2019 with data from archived samples collected in 2001 and 2009. Such a time series provides a crucial constraint for determining the trajectory of bomb-derived ^{14}C concentrations over time (Baisden et al., 2002; Stoner et al., 2021). Whether bomb-C concentrations are increasing or decreasing in bulk or respired CO_2 over time depends on both on the distribution of soil C among pools with different cycling rates as well as the year in which the soil was sampled (Beem-Miller et al., 2021). Given this, the trajectory of ^{14}C cannot be easily determined from observations at a single point in time (Baisden et al., 2013). Using the radiocarbon time series in combination with previously determined mineralogical data, we were able to test several hypotheses regarding the roles of mineralogical versus climatic factors in determining both overall cycling rates and the dynamics of transiently cycling soil C.

We can expect soils with large stocks of persistent soil C to have depleted values of $\Delta^{14}C_{bulk}$ relative to soils dominated by fast cycling soil C. If climate proves more important than parent material for determining soil C persistence, than we would expect to see large differences in $\Delta^{14}C_{bulk}$ among climate regimes when comparing soils within a given parent material, but minimal differences among parent materials when comparing soils within the same climate regime. However, if parent material proves more important than climate for soil C persistence, we would expect the opposite trends in $\Delta^{14}C_{bulk}$: differences would be greater among parent materials within a given climate regime than among climate regimes within a given parent material. Alternatively, if persistent soil C were associated with specific soil minerals, we would expect an interactive effect of parent material and climate on $\Delta^{14}C_{bulk}$. For example, if soil C persistence is due to the association of soil organic matter with PCMs, we would expect to observe the most depleted $\Delta^{14}C_{bulk}$ values where the combination of parent material and climate factors has led to the greatest abundance of these specific soil minerals.

Soil C found in association with minerals is typically older than organic matter found in free particulate forms (Lavallee et al., 2020). Accordingly, we might expect climate to be the dominant factor controlling the amount and cycling rates of C in transiently cycling soil C pools, with mineral factors being less relevant at these shorter timescales. If this hypothesis is correct, we would expect to see greater differences in $\Delta^{14}C_{respired}$ among different climate regimes and within a given parent material than we would among different parent materials within the same climate regime. Furthermore, given sufficient moisture, we would expect warmer climate soils to have $\Delta^{14}C_{respired}$ values closer to the atmosphere than colder climate soils, due to faster decomposition rates in the actively cycling soil C pools. Accordingly, we would also expect $\Delta^{14}C_{respired}$ to change more over time at the warmer climate sites than at the colder climate sites.

2. Methods

2.1 Site descriptions

We collected samples from nine sites in the Sierra Nevada Mountains of California (see Rasmussen et al., 2018b for a map of sampling locations). Parent material changes from basalt to andesite to granite along the north-south axis of the cordillera,

while MAT decreases as a function of increasing elevation along the east-west axis (Table 1). Total mean annual precipitation (MAP) ranges from 910 to 1400 mm yr^{-1} across the sites. Precipitation increases slightly with elevation (Table 1), and falls mainly as rain at lower elevations (< 1400 m), but mainly as snow at higher elevations (> 1800 m) (Rasmussen, 2004). The andesitic and basaltic parent materials receive slightly more precipitation on average than the granitic soils, with MAP of 1330 (± 75) mm yr^{-1}, 1160 (± 175) mm yr^{-1}, and 1000 (± 85) mm yr^{-1} averaged across the andesite, basalt, and granite transects, respectively.

Vegetation at the study sites is typical of the Sierran Mixed Conifer habitat (Parker and Matyas, 1981). All of the sites are forested and dominated by conifers. The species composition changes along the elevation and climate gradient, but not along the parent material gradient. Tree species at the lowest elevation warm climate sites are predominantly *Pinus ponderosa* mixed with lesser amounts of *Quercus* spp. The canopy species at the mid-elevation cool climate sites consist primarily of *Abies concolor* and *Pinus lambertiana*, while *Abies magnifica* dominates at the high elevation cold climate sites. Species present at all sites include *Calocedrus decurrens* in the canopy, the shrubs *Arctostaphylos* spp., *Chamaebatia foliolosa*, and *Ceanothus* spp. in the understory, and variable ground cover of grasses and forbs.

2.2 Sample collection

Site locations were initially established in 2001 by C. Rasmussen (Rasmussen, 2004) and resampled in 2009 (Rasmussen et al., 2018b) and 2019 (this study). Three replicate pits were dug at each site. Samples were collected from the A horizon only in 2001, and from both the A and B horizons in 2009 and 2019. Sampling was done from pit sidewalls by horizon in 2001 and 2009, and by 0.1 m increments in 2019. We relocated the sites for the 2019 sampling using GPS and geospatial coordinates recorded during site establishment. Prior to sample collection we compared the soil profiles to the pedon descriptions from the 2001 sampling campaign to confirm the profiles matched. While deeper samples were collected in 2009 and 2019, we focus on the upper mineral soil layers in this study (0 to ca. 0.3 m) as the 2001 sampling was restricted to this depth range.

2.3 Incubations

Laboratory soil incubations were performed on composite samples from the three replicate profiles sampled at each site in 2001 and 2019. We omitted the 2009 samples from the incubation experiment to save on time and analysis costs, and because sample material was only available from a single profile at each site. We composited and incubated each depth increment separately in 1 L glass mason jars fitted with airtight sampling ports in the lids. Incubations were performed in duplicate. Prior to the start of incubations, we adjusted the soil moisture content to 60% of water holding capacity (WHC). Samples from 2001 were air-dried prior to archiving, and therefore we also air-dried the freshly collected soils from 2019 in order to control for the known effects of drying and rewetting on $\Delta^{14}C_{respired}$ (Beem-Miller et al., 2021). We defined WHC as

the gravimetric water content of water-saturated soil placed in mesh-covered (50µm) tubes (50ml) weighed after draining for 30 minutes on a bed of fine sand. Following rewetting we allowed the soils to respire for one week before closing the jars.

Table 1. Soil and climate data by site.

					pH[1]		Sand[1]		Clay[1]		
Parent Material	Climate Zone	MAT	MAP	Elev	mean	range	mean	range	mean	range	Soil Taxonomy[2]
		°C	*mm yr^{-1}*	*masl*			*g kg^{-1}*		*g kg^{-1}*		*USDA-NRCS*
andesite	warm	11.5	1250	1167	6.4	(6.3, 6.4)	384	(352, 410)	323	(264, 342)	fine, parasesquic, mesic, Andic Palehumult
	cool	8.5	1400	1737	6.2	(6.1, 6.3)	608	(589, 617)	58	(43, 64)	medial-skeletal, amorphic, mesic Humic Haploxerand
	cold	6.0	1350	2240	5.8	(5.7, 6.0)	613	(605, 618)	52	(47, 64)	medial-skeletal, amorphic, frigid Humic Vitrixerand
basalt	warm	13.3	990	1167	5.9	(5.8, 6.2)	354	(343, 367)	272	(263, 280)	fine, kaolinitic, mesic Xeric Haplohumult
	cool	8.3	1150	1737	6.5	(6.4, 6.6)	797	(670, 853)	104	(70, 116)	loamy-skeletal, mixed, superactive, mesic Typic Haploxerept
	cold	6.5	1340	2240	6.0	(5.9, 6.3)	768	(680, 930)	57	(37, 65)	sandy-skeletal, mixed, superactive, frigid Typic Xerorthent
granite	warm	11.1	910	1385	5.8	(5.6, 5.8)	615	(601, 622)	153	(143, 160)	fine-loamy, mixed, semiactive, mesic Ultic Haploxeralf
	cool	9.1	1010	1789	6.1	(6.0, 6.1)	824	(800, 829)	62	(47, 67)	coarse-loamy, mixed, superactive, mesic Humic Dystroxerept
	cold	7.2	1080	2317	5.5	(5.4, 5.5)	810	(810, 811)	40	(40, 40)	mixed, superactive, frigid Dystric Xeropsamment

Abbreviations: MAP—mean annual precipitation; MAT—mean annual temperature; Elev—elevation; masl—meters above sea level. [1] pH and particle size data are from samples collected in 2009 and aggregated over the depth increment 0–0.3 m. Data were aggregated using a mass-weighted spline function (see text for details). [2] Soil taxonomy previously reported in Rasmussen et al. (2018b).

Incubations proceeded until CO_2 concentrations in the jar headspace reached approximately 10,000 ppm, at which point we collected a 400 ml gas subsample for radiocarbon analysis. Gas samples were collected with pre-evacuated stainless-steel vacuum canisters (Restek GmbH, Bad Homburg, Germany). All incubations were performed in the dark at 20°C.

2.4 Soil Physical Analyses and Mineral Characterization

Data on soil particle size distribution, bulk density, and mineral characterization were obtained from previously published analyses of samples collected at the study sites in 2001 and 2009 (Rasmussen et al., 2005, 2007, 2010a, b, 2018b). Both qualitative and quantitative approaches were used to characterize soil mineral assemblages, including X-ray diffraction (XRD) for the clay (<2 μm) fraction, and non-sequential selective dissolution. These previous analyses revealed that the dominant mineral species in the soils of the highly weathered warm climate zone were similar across parent materials, but differed substantially across parent materials at the less weathered cool and cold climate sites. Mineral assemblages at the warm climate sites are dominated by 1:1 clays and large accumulations of crystalline iron oxides (Dahlgren et al., 1997; Rasmussen et al., 2010a, b). In contrast, the cool and cold climate andesitic soils contain high concentrations of poorly crystalline short-range order (SRO) minerals such as allophane and iron oxyhydroxides. The cool and cold climate basaltic soils contain intermediate amounts of SRO minerals, while the granitic soils lack SRO minerals almost entirely, but are rich in quartz and contain relatively more hydroxyl-interlayered vermiculite than soils from the other lithologies (Rasmussen, 2004).

The previous work at these sites showed that the PCM content was the best predictor of both C abundance and $\Delta^{14}C_{bulk}$ (Rasmussen et al., 2018b). Accordingly, our analyses focus on the relationship between radiocarbon measurements and the abundance of PCMs versus CRMs rather than the whole suite of mineralogical data. For simplification, we use the sum of ammonium-oxalate extractable aluminum and half of the ammonium-oxalate extractable Fe selectively dissolved from bulk soils as a proxy for the abundance of PCMs (including poorly and non-crystalline metal oxides), and the difference of dithionite-citrate extractable Fe and ammonium-oxalate extractable Fe as a proxy for CRM abundance (Kleber et al., 2005).

2.5 Carbon, Nitrogen, and Radiocarbon Analysis

Total carbon content was determined by dry combustion (2019 samples: Vario Max, Elementar Analysensysteme GmbH, Langenselbold, Germany) on finely ground soils (2019 samples: MM400, Retsch GmbH, Haan Germany). For radiocarbon analysis of 2001 and 2019 samples, we first purified CO_2 from combusted soil samples (bulk soils) and incubation flask samples (respired CO_2) on a vacuum line using liquid N_2. Following purification, samples were graphitized with an iron catalyst under an H_2 enriched atmosphere at 550 °C. Radiocarbon content was then measured by accelerator mass spectrometry (Micadas, Ionplus, Zurich, Switzerland) at the Max Planck Institute for Biogeochemisty (Steinhof et al., 2017). See Rasmussen et al. (2018b) for details of C and radiocarbon analysis of the 2009 samples.

We report radiocarbon values using units of $\Delta^{14}C$, defined as the deviation in parts per thousand of the ratio of $^{14}C/^{12}C$ from that of the oxalic acid standard measured in 1950. This unit also contains a correction for the potential effect of mass-dependent fractionation by normalizing sample $\delta^{13}C$ to a common value of -25 per mil (Stuiver and Polach, 1977). Values of $\Delta^{14}C > 0$ indicate the presence of 'bomb' C produced by atmospheric weapons testing in the early 1960s; values of $\Delta^{14}C < 0$ indicate radioactive decay of ^{14}C, which has a half-life of 5730 years.

2.6 Spline fitting

We used a spline function to compare soil properties from samples collected from different depth intervals in different years and at different sites. We were motivated to use consistent depth increments across sites when resampling in 2019 because of the strong correlation between depth and $\Delta^{14}C$ observed in the 2009 dataset, a correlation also noted in numerous other studies (Mathieu et al., 2015; Shi et al., 2020). We fit a mass-preserving quadratic spline to the 2001 and 2009 profiles in order to convert soil property data to the equivalent depth increments sampled in 2019 (Bishop et al., 1999). We performed the spline fitting with the mpspline function of the GSIF package in R, using a λ value of 0.1 (Hengl, 2019).

2.7 Statistical analysis

We used a linear modeling approach to assess the relative explanatory power of climate versus parent material on the observed variation in $\Delta^{14}C$, as well as potential interactions between these two factors. We constructed separate models for $\Delta^{14}C_{bulk}$ and $\Delta^{14}C_{respired}$ but with the same equation structure (Eq. (1)). For each model we considered the two-way interaction between parent material and climate as well as the three-way interaction with time. For ease of interpretation, we considered the effect of depth by modeling each depth layer separately (0–0.1 m, 0.1–0.2 m, 0.2–0.3 m). We also made pairwise comparisons of $\Delta^{14}C_{bulk}$ and $\Delta^{14}C_{respired}$ across sites and within years, and across years for individual sites. We assessed the significance of the temporal trend for pairwise combinations of parent material and climate using the emmtrends function of the emmeans package (Lenth, 2021). We corrected for multiple comparisons using Tukey's honestly significant mean difference.

$$\Delta^{14}C = \alpha + \beta_1(Parent\_material) \times \beta_2(Climate) \times \beta_3(Year) + \varepsilon\,, \quad (1)$$

where α is the intercept term, the β terms are coefficients, and ε is random error.

We also considered the relationship between $\Delta^{14}C_{bulk}$ and $\Delta^{14}C_{respired}$ in order to gain insight into potential differences in soil C dynamics and persistence mechanisms across our sites (Sierra et al. 2018). We modeled the effects of parent material Eq. (2) and climate Eq. (3) on this relationship separately, as we did not have an adequate number of observations to consider the interactions. For this analysis, we used $\Delta^{14}C$ measurements made on samples collected in 2001 and 2019, and data from all depths. We excluded both depth and time from the models as the three-way interactions between depth or time, $\Delta^{14}C_{bulk,}$ and the explanatory variable (parent material in Eq. (2), or climate in Eq. 3) were not significant ($\alpha = 0.1$).

$$\Delta^{14}C_{respired} = \alpha + \beta_1(\Delta^{14}C_{bulk}) \times \beta_2(Parent\_material) + \epsilon \quad (2)$$

$$\Delta^{14}C_{respired} = \alpha + \beta_1(\Delta^{14}C_{bulk}) \times \beta_2(Climate) + \epsilon \quad (3)$$

We assessed the relative importance of PCMs versus CRMs in protecting soil C from microbial decomposition by regressing $\Delta^{14}C$ against the concentrations of ammonium-oxalate extractable iron, ammonium-oxalate extractable aluminum, pyrophosphate extractable aluminum, and dithionite-citrate extractable iron (Eq. 4). We fit the model for $\Delta^{14}C_{bulk}$, $\Delta^{14}C_{respired}$, and the difference between $\Delta^{14}C_{respired}$ and $\Delta^{14}C_{bulk}$ ($\Delta^{14}C_{bulk\text{-}respired}$). We used $\Delta^{14}C$ data from 2001, 2009, and 2019 for the $\Delta^{14}C_{bulk}$ model, but only data from 2001 and 2019 for the $\Delta^{14}C_{respired}$ and $\Delta^{14}C_{bulk\text{-}respired}$ models (as $\Delta^{14}C_{respired}$ data were not available for the 2009 samples). Selective dissolution was only performed on the soils collected in 2001, but these data were assumed to be comparable for the other time points as they reflect weathering processes operating at timescales much beyond the 18-year duration of this study. The regression analysis conducted with Eq. (4) was done for the combined depth increment of 0–0.3 m, as extracted metal concentrations did not change substantially over this depth (Rasmussen et al., 2018b). Combining depth increments allowed us to control for the depth dependence of $\Delta^{14}C$ as well as to simplify interpretation of the data. In order to obtain values for the necessary data over the 0 to 0.3 m depth increment we computed mass-weighted estimates of extractable metal concentrations, carbon mass-weighted means of $\Delta^{14}C_{bulk}$, and flux-weighted means of $\Delta^{14}C_{respired}$; these calculations were made prior to determining $\Delta^{14}C_{bulk\text{-}respired}$.

$$\Delta^{14}C = \alpha + \beta_1(Metal_x) + \beta_2(time) + \varepsilon, \quad (4)$$

where α is the intercept term, β is the coefficient for each factor in the model, $Metal_x$ is the concentration of selectively dissolved metal oxides, time is the year of sampling, and ε is random error.

We present the results of regression analyses looking at PCMs versus CRMs in the main text (§3.5, Fig. 5). Results for specific relationships between the concentration of Fe or Al extracted with ammonium-oxalate, Fe extracted with dithionite-citrate, and Al extracted with sodium-pyrophosphate, and $\Delta^{14}C_{bulk}$, $\Delta^{14}C_{respired}$, and the difference between $\Delta^{14}C_{respired}$ and $\Delta^{14}C_{bulk}$ ($\Delta^{14}C_{respired\text{-}bulk}$) are provided in the supplemental information (SI §5, SI Figs. 4–6).

3 Results

3.1 Soil carbon concentrations and flux rates

We observed both parent material and climate effects on soil organic C (SOC) concentration (Fig. 1a–c). Concentrations of SOC were similar among parent materials for the warm climate sites (Fig. 1a), while at the cool and cold climate sites (Fig. 1b, c) the andesitic soils had higher SOC concentrations than either the basaltic or granitic soils. The basaltic and granitic soils had similar SOC concentrations across climate zones, while the cool and cold climate andesitic soils were enriched in C relative to the warm climate soils. Soils showed a similar decrease in SOC concentration with depth across all sites (Fig. 1).

We did not calculate SOC stocks for the 2019 samples as we did not measure bulk density or coarse fragment content for these samples (Schrumpf et al., 2013; Beem-Miller et al., 2016). However, measurements of SOC stocks made in 2001 and 2009 showed similar overall trends as SOC concentration, with the highest SOC stocks observed in the andesitic soils, followed by the basalt and granitic soils for which SOC stocks were similar (Fig. 1d–f, see also Rasmussen et al., 2018b).

Soil organic C concentrations did not change significantly over time at the majority of our sites (SI Fig. 1). We saw the most substantial variation in SOC concentration between 2001, 2009, and 2019 in the surface mineral layers (0–0.1 m). We observed significant differences between years for the 0–0.1 m layer at the warm climate andesitic and basaltic sites, and for 0–0.1 m, 0.1–0.2 m, and 0.2–0.3 m layers at the cold climate andesitic site (SI Table 1).

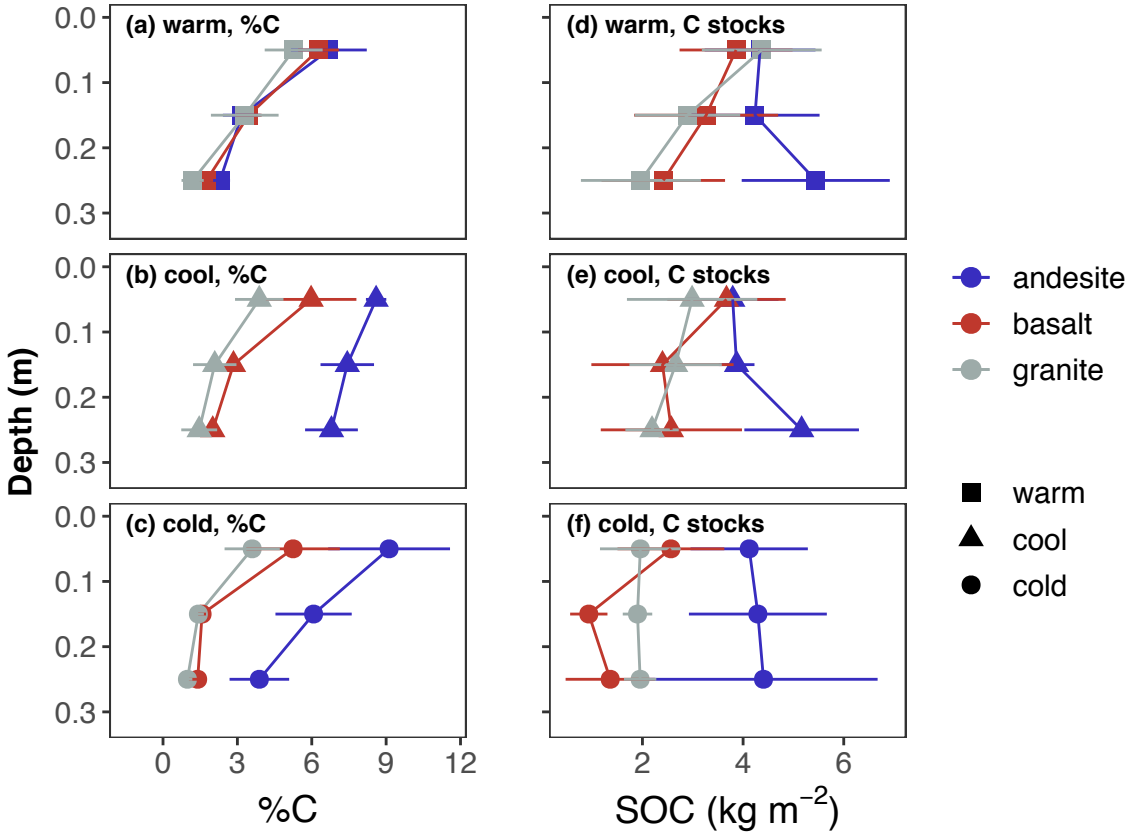

Figure 1. Profiles of SOC concentration (a–c) and stocks (d–f). Points show mean of 2001, 2009, and 2019 data for SOC concentration, and 2001 and 2009 data for SOC stocks (bulk density was not measured in 2019); error bars show ±2SE.

Flux rates of heterotrophic respiration differed among parent materials and among climate zones. When compared on a carbon basis (mg CO_2 g C^{-1} d^{-1}), flux rates tended to be higher for the andesitic soils than soils from either basaltic or andesitic soils, particularly at depth (SI Fig. 2). The exceptions to this trend were the surface (0–0.1 m, 2001 and 2019) and

near-surface (0.1–0.2 m, 2019) soils from the warm climate sites (SI Fig. 2). Respiration rates for granitic and basaltic soils tended to decrease with decreasing MAT (warm > cool > cold); however, we did not see any clear trend in respiration rates with respect to climate for the andesitic soils (SI Fig. 2).

3.2 Radiocarbon depth profiles

3.2.1 Bulk soil.

$\Delta^{14}C_{bulk}$ covaried with both parent material and climate. We observed the most enriched $\Delta^{14}C_{bulk}$ at the warm climate sites, indicating a preponderance of relatively young, fast-cycling C in these soils. However, contrary to what would be expected from the decomposition-temperature relationship, we observed the oldest soil C (i.e. most depleted $\Delta^{14}C_{bulk}$ values) at the cool climate sites with intermediate MAT (Fig. 2b) rather than at the cold climate sites (Fig. 2c). When comparing $\Delta^{14}C_{bulk}$ from different parent materials within a given climate zone, $\Delta^{14}C_{bulk}$ of andesitic soils tended to be the most depleted, while the granitic soils tended to be the most enriched (Fig. 2a–c; SI Tables 2–4). We focus here on the 2019 data for simplicity, but $\Delta^{14}C_{bulk}$ profiles showed similar patterns in both 2001 (SI Fig. 3a) and 2009 (Rasmussen et al., 2018b).

Analysis of variance for $\Delta^{14}C_{bulk}$ revealed significant two-way interactions between parent material and climate at all depths (Table 2). This interaction was evident in the differences in $\Delta^{14}C_{bulk}$ that we observed among parent materials within each climate zone. We observed the greatest differences in $\Delta^{14}C_{bulk}$ among parent materials at the warm and cool sites (Fig. 2a, b), while $\Delta^{14}C_{bulk}$ was similar among parent materials at the coldest sites (Fig. 2c). We also found depth to be an important factor influencing the relative importance of climate versus parent material effects on $\Delta^{14}C_{bulk}$. Although $\Delta^{14}C_{bulk}$ declined with depth for all sites, climate explained more of the variance in $\Delta^{14}C_{bulk}$ in the uppermost soil layer (0–0.1 m) whereas parent material explained more in the bottom two layers (0.1–0.2 m, 0.2–0.3 m) (Table 2).

3.2.2 Heterotrophically respired CO_2.

The patterns we observed in $\Delta^{14}C_{respired}$ were similar to those we observed in $\Delta^{14}C_{bulk}$ (Fig. 2d–f). We found climate to the only significant factor for explaining the variance observed in $\Delta^{14}C_{respired}$ in the uppermost soil layer (0–0.1 m), while at the deepest depth (0.2–0.3 m) parent material was more important than climate (Table 2). Overall, we found the two-way interaction between parent material and climate explained more of the variance in $\Delta^{14}C_{respired}$ than it did in $\Delta^{14}C_{bulk}$ (Table 2).

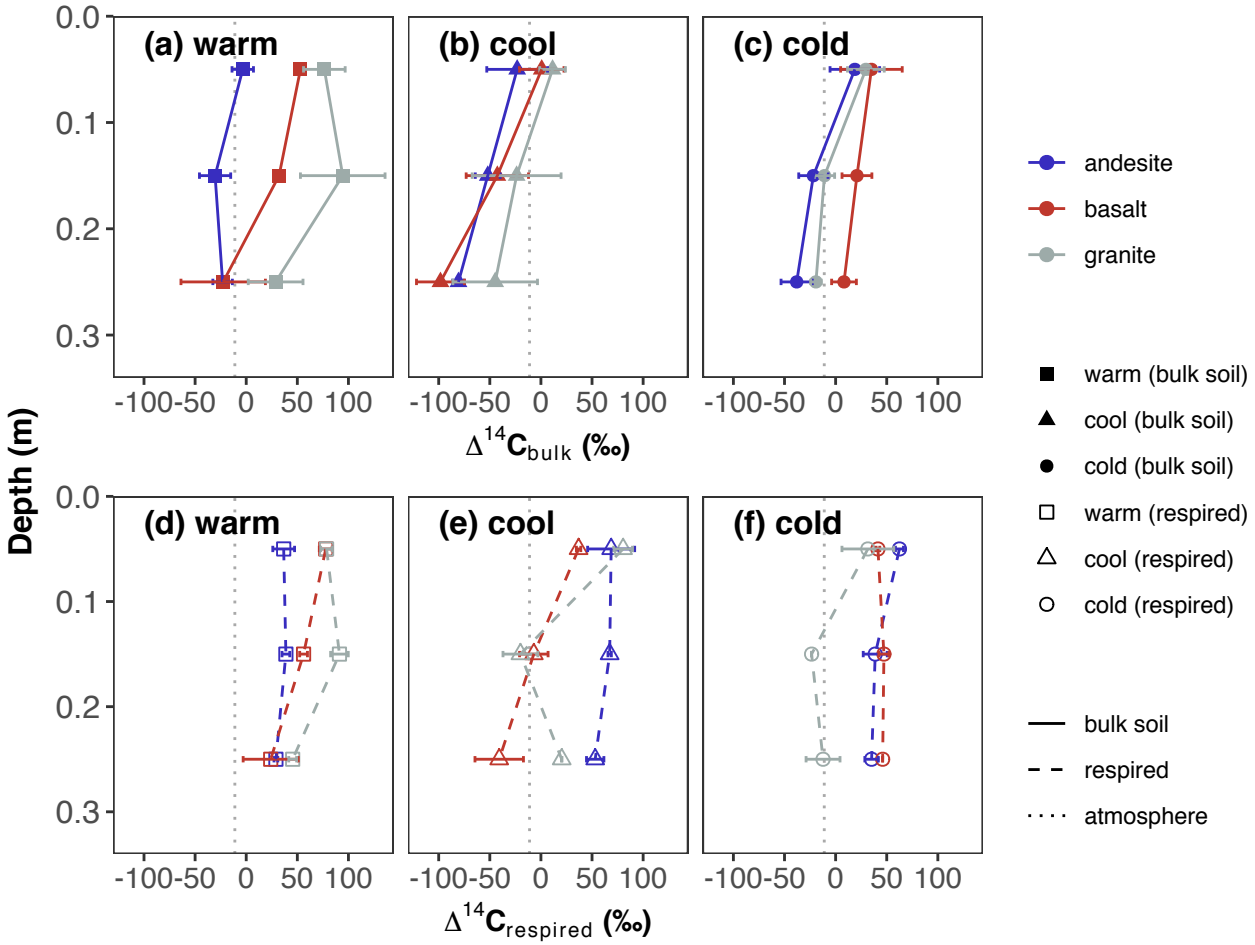

Figure 2. Depth profiles of $\Delta^{14}C_{bulk}$ (a–c) and $\Delta^{14}C_{respired}$ (d–f) in 2019. Points show the mean of three replicate profiles for bulk soil, and the mean of laboratory duplicates for respired CO_2. Error bars show ±1 SD for bulk soils and the minimum and maximum for respired CO_2. Dotted gray vertical line shows $\Delta^{14}C$ of the atmosphere in the year of sampling, 2019 (data from Graven et al. 2017, forecasted to 2019 using the method of Sierra 2018).

The effect of climate on $\Delta^{14}C_{respired}$ was moderated by parent material. Accordingly, we did not observe significant differences in $\Delta^{14}C_{respired}$ among the andesitic soils when compared across climate zones at any depth (SI Tables 2–4). In contrast, $\Delta^{14}C_{respired}$ diverged substantially between climate zones for the basaltic and granitic soils, particularly for the 0.1–0.2 m and 0.2–0.3 m depth layers (Fig. 2d–f). Overall, $\Delta^{14}C_{respired}$ values across sites were most similar at the soil surface (0–0.1 m), and most divergent at the intermediate depth (0.1–0.2 m) (Fig. 2d–f).

3.3 Radiocarbon time series

Temporal trends in bulk and respired $\Delta^{14}C$ reflect the degree to which soil C is exchanging with C fixed from the atmosphere. The average annual decline in $\Delta^{14}C$ atmospheric CO_2 between 2001 and 2009 for the northern hemisphere was -5.13 per mil yr^{-1} (Graven et al., 2017; Sierra, 2018) (Fig. 3, dotted lines). Therefore, changes in $\Delta^{14}C$ of soil C that parallel the atmospheric trend must be exchanging relatively rapidly compared to those that change little over the same time period.

3.3.1 Bulk soil

We observed a significant three-way interaction between parent material, climate, and time at all three depths in the linear models (Eq. 1) for $\Delta^{14}C_{bulk}$ (Table 2). The change over time in $\Delta^{14}C_{bulk}$ was also affected by depth, with greater differences seen between 2001 and 2019 in the uppermost soil layer than in the deeper layers (Fig. 3a–f). We observed a significant decrease in $\Delta^{14}C_{bulk}$ over time in both warm and cool climate granitic soils for the uppermost soil layer (0–0.1 m), and additionally for the warm climate andesitic soils (Fig. 3a, c; SI Table 5). In the deeper soil layers (0.1–0.2 m and 0.2–0.3 m), we only observed a significant change over time in $\Delta^{14}C_{bulk}$ for the cool climate basalt and granite soils (Fig. 3d, 0.2–0.3 m data not shown; SI Table 5). $\Delta^{14}C_{bulk}$ of the cool climate andesitic soils remained essentially unchanged between 2001 and 2019 for all depths (Fig. 3c, d; SI Table 5), underscoring the importance of the interaction between parent material and climate for explaining temporal trends in $\Delta^{14}C_{bulk}$.

The relationship of $\Delta^{14}C_{bulk}$ to atmospheric $\Delta^{14}C$ also depended on the combination of parent material and climate. In 2001, the warm climate sites were the only sites where the basaltic and andesitic soils were enriched relative to the atmosphere, and this enrichment was only observed for the uppermost soil layer (Fig. 3a). In contrast, 0–0.1 m layer granitic soils at both the warm and cool climate sites were enriched relative to the atmosphere in 2001 (Fig. 3a, c). For the cold climate sites, where $\Delta^{14}C_{bulk}$ was most similar, all three lithologies were depleted relative to atmospheric in both surface and subsoil layers in 2001 (Fig. 3e, f).

We observed that $\Delta^{14}C_{bulk}$ remained either unchanged or tended to decrease between 2001 and 2019 across sites. In the latter case, the rates of change in $\Delta^{14}C_{bulk}$ were typically smaller than the corresponding change in atmospheric $\Delta^{14}C$ over the same period. Accordingly, $\Delta^{14}C_{bulk}$ measured in 2019 tended to be enriched relative to the atmosphere at more sites, and also more enriched at depth than in 2001. We observed surface soil $\Delta^{14}C_{bulk}$ (0–0.1 m) in 2019 to be enriched relative to the atmosphere at all sites except for the cool climate andesite soils (Fig. 3; Fig. 2d–f). Furthermore, $\Delta^{14}C_{bulk}$ was enriched relative to the atmosphere down to 0.3 m at two of the sites in 2019: the warm climate granite soil (Fig. 2d) and cold climate basalt soil (Fig. 2f). $\Delta^{14}C_{bulk}$ at the cool climate andesite site was the most depleted relative to the atmosphere at all time points (Fig. 3c, d).

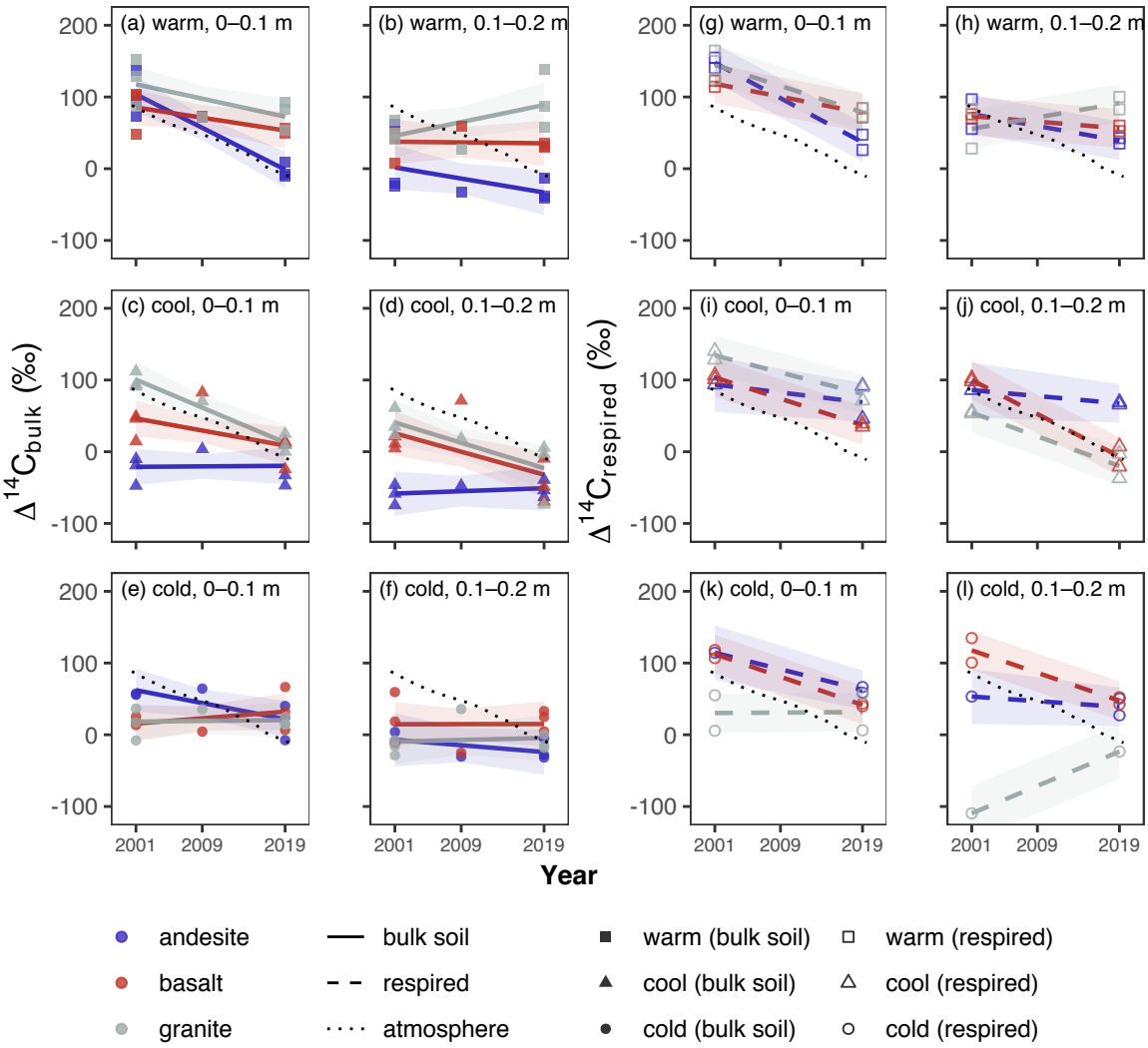

Figure 3. Temporal trends in $\Delta^{14}C$ for 0–0.1 m and 0.1–0.2 m depth layers. Panels (a–f) show $\Delta^{14}C_{bulk}$ data. The first column from left—panels (a), (c), and (e)—shows 0–0.1 m data; the second column—panels (b), (d), and (f)—shows 0.1–0.2 m data. Panels (g–l) show $\Delta^{14}C_{respired}$ data; the third column—panels (g), (i), and (k)—shows 0–0.1 m data; the rightmost column—panels (h), (j), and (l)—shows 0.1–0.2 m data. Points show observed data; lines show linear trend estimates for marginal means; ribbons show 95% confidence intervals for trends. Dotted line shows atmospheric $\Delta^{14}C$ (data from Graven et al. 2017, forecasted to 2019 using the method of Sierra 2018).

3.3.2 Heterotrophically respired CO_2.

Temporal trends in $\Delta^{14}C_{respired}$ (Fig. 3g–l) tended to be of greater magnitude than what we observed for $\Delta^{14}C_{bulk}$ (Fig. 3a–f). However, changes in $\Delta^{14}C_{respired}$ between 2001 and 2019 still tended to be smaller in magnitude than the change observed in

the atmosphere over this period (Fig. 3g–l). In contrast to $\Delta^{14}C_{bulk}$, $\Delta^{14}C_{respired}$ values of both surface and near surface soils (0–0.2 m) were close to atmospheric levels in 2001, while in 2019, $\Delta^{14}C_{respired}$ tended to be enriched relative to the atmosphere, even for the deeper soil layers (Fig. 3g–l).

We saw significant decreases in $\Delta^{14}C_{respired}$ over time for surface (0–0.1 m) soils at seven of the nine sites, with the only exceptions being the cool climate andesitic and cold climate granitic sites (Fig. 3, g–l; SI Table 6). In absolute terms, the changes in $\Delta^{14}C_{respired}$ over time in the uppermost soil layer were greatest at the warm sites (-4 ±2 per mil yr^{-1}), while changes were similar for the cool and cold sites (-2.7 ±1.2 per mil yr^{-1}, and -2.2 ±2.1 per mil yr^{-1}, respectively). When considered within parent materials, granitic soils showed the greatest decrease in $\Delta^{14}C_{respired}$ over time at the warm climate site and the least change at the cold climate site. In contrast, the andesitic soils showed the least amount of change over time at the cool climate sites, and changes over time in the basaltic soils were similar across all three of the climate zones (Fig. 3g–l).

The magnitude of the change in $\Delta^{14}C_{respired}$ over time tended to decrease with depth for all soils (Fig. 3g–l). For the 0.1–0.2 m layer, we observed significant negative trends over time for $\Delta^{14}C_{respired}$ at only four of the nine sites (warm andesite, cool basalt, cool granite, and cold basalt) (Fig. 3h, j, l; SI Table 6), and only one site for the 0.2–0.3 m layer (cold basalt) (SI Table 3). $\Delta^{14}C_{respired}$ at the cool andesitic soils remained unchanged at all depths over the study period (Fig. 3g–l; SI Table 6).

Table 2. ANOVA for $\Delta^{14}C_{bulk}$ and $\Delta^{14}C_{respired}$[1]

		Bulk soil			Respiration		
Depth	Predictor	*df*	*F*	*p*	*df*	*F*	*p*
0–0.1 m	Parent material	2	12.00	**< 0.001**	2	0.04	0.958
	Climate	2	32.34	**< 0.001**	2	14.02	**< 0.001**
	Year	1	32.03	**< 0.001**	1	75.29	**< 0.001**
	Parent material:Climate	4	8.75	**< 0.001**	4	7.9	**0.001**
	Parent material:Year	2	2.38	0.105	2	1.93	0.177
	Climate:Year	2	6.61	**0.003**	2	2.26	0.137
	Parent material:Climate:Year	4	5.19	**0.002**	4	3.75	**0.024**
	Residuals	44			44		
0.2–0.3 m	Parent material	2	15.58	**< 0.001**	2	0.92	0.421
	Climate	2	11.61	**< 0.001**	2	0.77	0.483
	Year	1	1.30	0.260	1	0.65	0.434
	Parent material:Climate	4	1.71	0.165	4	4.33	**0.019**
	Parent material:Year	2	1.56	0.222	2	0.86	0.446
	Climate:Year	2	4.04	**0.024**	2	1.41	0.278
	Parent material:Climate:Year	4	0.98	0.430	2	0.37	0.698
	Residuals	44			44		

[1]Bold text indicates significance at $\alpha < 0.05$.

We observed a significant increase in $\Delta^{14}C_{respired}$ from 2001 to 2019 at only one site: the cold climate granitic soil (Fig. 3l; SI Table 6). This was also the only soil for which $\Delta^{14}C_{respired}$ was more depleted than $\Delta^{14}C_{bulk}$. We observed this anomaly for the deeper soil layers in both 2001 and 2019. We measured $\Delta^{14}C_{respired}$ values of -469 and -127 per mil for the 0.08–0.27 m layer in 2001, compared to $\Delta^{14}C_{bulk}$ values of -31 and -11 per mil in the same year. Similarly, we observed $\Delta^{14}C_{respired}$ values of -397 and -24 per mil for the 0.1–0.2 m layer in 2019, compared to -18 and 0 per mil for $\Delta^{14}C_{bulk}$. However, these anomalous values of $\Delta^{14}C_{respired}$ were restricted to the deeper soil layers from this one site, and were consistent over time, thus the response appears to be artifact that is unique to these soils. If old soil C dominated the release flux in situ, it would indicate the C dynamics of the system were not in equilibrium, which we think unlikely. We suspect this phenomenon is related to disturbance of the soil during sample extraction and preparation, and accordingly, we have excluded these highly depleted samples from the statistical analyses.

3.4 Relationship of bulk soil and respired CO_2 $\Delta^{14}C$

We assessed the relationship between $\Delta^{14}C_{bulk}$ and $\Delta^{14}C_{respired}$ using linear regression models for parent material Eq. (3) and climate Eq. (4). We observed that while $\Delta^{14}C_{respired}$ was enriched relative to $\Delta^{14}C_{bulk}$ for almost all sites and all depths, the magnitude of the difference depended on both parent material and climate. Accordingly, y-intercepts for all models were indistinguishable from or greater than zero, indicating that CO_2 respired by these soils is predominantly modern (i.e. < 60 years old) in all but the deepest soil layers, regardless of parent material or climate regime. We found the largest y-intercept values for the soils developed on andesitic parent material (72 per mil), and for soils in the cool climate zones (65 per mil), values indicating that CO_2 respired from these soils is relatively enriched in decadally cycling bomb-C.

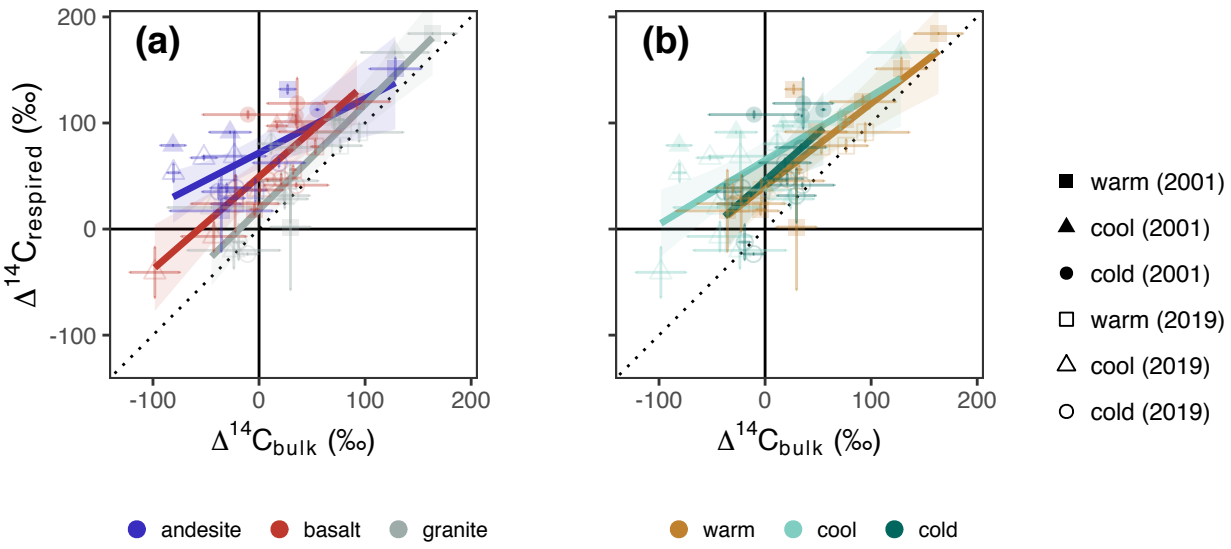

Figure 4. Parent material and climate effects on the relationship of $\Delta^{14}C_{bulk}$ and $\Delta^{14}C_{respired}$. (a) Parent material model, Eq. (3) and (b) Climate model, Eq. (4). Dotted line shows 1:1 relationship. Points show the mean of three replicate profiles for $\Delta^{14}C_{bulk}$, and the mean of laboratory duplicates for $\Delta^{14}C_{respired}$. Error bars show ±1 SD for $\Delta^{14}C_{bulk}$, and the minimum and maximum for $\Delta^{14}C_{respired}$. The cold granite site in 2001 had extremely depleted in $\Delta^{14}C_{respired}$ values and thus was from the models.

Slope values less than one in these models indicate that every per mil change in $\Delta^{14}C_{bulk}$ is associated with a correspondingly smaller change in $\Delta^{14}C_{respired}$. This suggests that the process regulating persistence of soil C on long time scales is distinct from that which regulates more transiently cycling soil C. Similar to what we found for the y-intercepts, modeled slopes for the parent material-only model (Eq. 2) were smallest for the andesitic soils: slope = 0.51, 95% CI = [0.22, 0.80]) (Fig. 4a), and for cool climate soils in the climate-only model (Eq. 3): slope = 0.61, 95% CI = [0.30, 0.91]) (Fig. 4b). While we could not test the interaction of parent material and climate factors in these models directly owing to the limited number of observations, we observed that mean differences in $\Delta^{14}C_{bulk}$ and $\Delta^{14}C_{respired}$ were substantially greater for the cool climate soils developed on andesitic parent material than for the other sites.

3.5 Mineral assemblages and radiocarbon

Mineral assemblage data is reported fully in Rasmussen et al. (2018). Here we focus on the selective dissolution data with respect to the trends we observed in $\Delta^{14}C_{bulk}$, $\Delta^{14}C_{respired}$, and $\Delta^{14}C_{respired\text{-}bulk}$. We observed a significant negative correlation between $\Delta^{14}C_{bulk}$ and the concentration of oxalate extractable iron, oxalate extractable aluminum, and pyrophosphate extractable aluminum (SI Fig. 5). For simplicity, we focus here on the difference between PCMs (the sum of oxalate extractable iron and oxalate extractable aluminum) and CRMs (the difference of dithionite-citrate extractable iron and oxalate extractable iron) (SI Fig. 7).

The relationship between PCM abundance and $\Delta^{14}C_{bulk}$ was highly significant (p <0.001), but the relationship between CRM abundance and $\Delta^{14}C_{bulk}$ was not (SI Fig. 7). For $\Delta^{14}C_{respired}$, we observed a significant relationship with PCM abundance for the 2001 samples (p = 0.04), but not for the 2019 samples (SI Fig. 8). Accordingly, the combined set of 2001 and 2019 data was only marginally significant (p = 0.07). However, we did see a highly significant relationship between PCM abundance and $\Delta^{14}C_{respired\text{-}bulk}$ (Fig. 5a). As with $\Delta^{14}C_{bulk}$, there was no relationship with CRM abundance for either $\Delta^{14}C_{respired}$ (SI Fig. 8) or $\Delta^{14}C_{respired\text{-}bulk}$ (Fig. 5b).

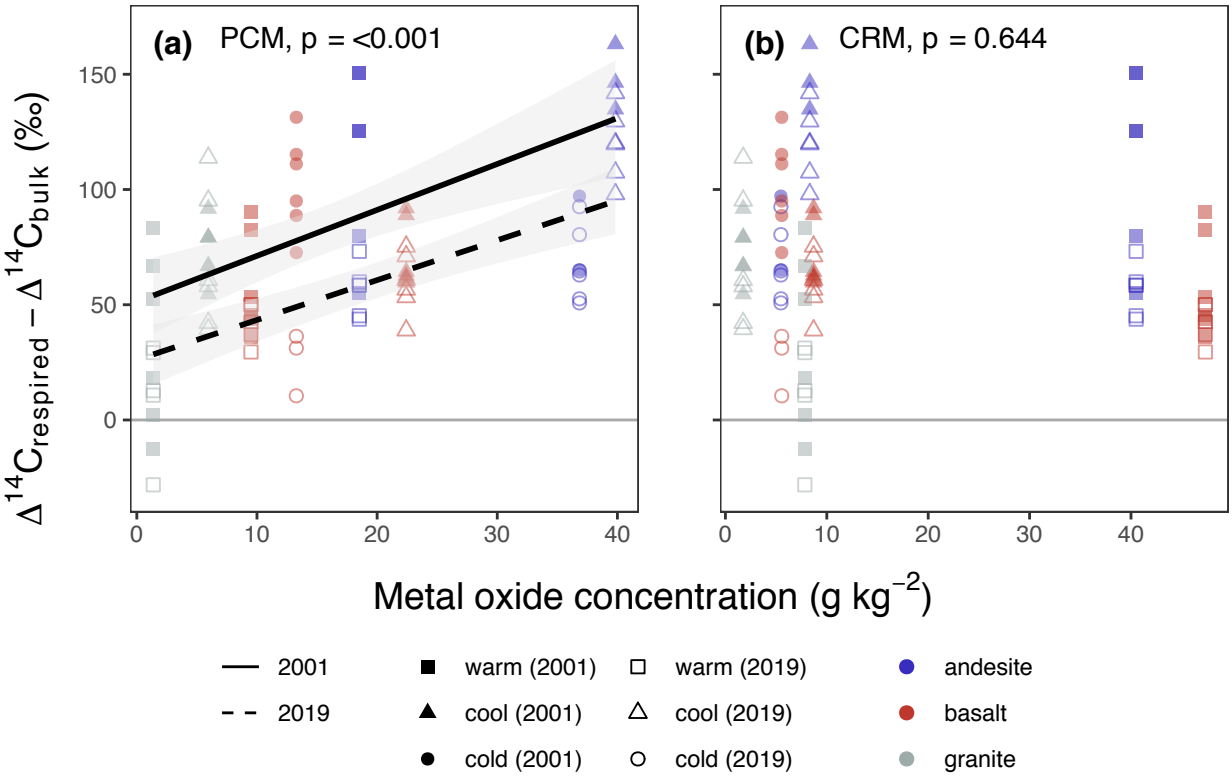

Figure 5. Relationship of poorly crystalline and crystalline metal oxides to the difference of $\Delta^{14}C_{respired}$ and $\Delta^{14}C_{bulk}$ ($\Delta^{14}C_{respired\text{-}bulk}$). (a) PCM = poorly crystalline metal oxide content (oxalate-extractable aluminum + 1/2 oxalate-extractable iron), (b) CRM = crystalline metal oxide content (dithionite-extractable iron - oxalate-extractable iron). Points show mass-weighted metal oxide concentrations and carbon-weighted values of $\Delta^{14}C_{respired\text{-}bulk}$ for 0–0.3 m profiles. Lines show partial slopes for 2001 and 2019 from the linear model fit (Eq. 5). P-values indicate significance of metal concentration coefficient estimate for predicting $\Delta^{14}C_{respired\text{-}bulk}$.

4 Discussion

Climatic and mineralogical factors both play key roles in soil carbon persistence. However, the relevance of parent material for explaining soil organic matter persistence in soils with mixed mineralogies is still poorly explained. In the current study we illuminate how parent material interactions with climate lead to the development of distinct mineral assemblages, which in turn control the dynamics of soil C cycling at timescales ranging from annual to centennial. Our key findings are 1) soil mineral characteristics mediate climatic controls on soil C cycling, and 2) mineralogical controls on soil C cycling are not limited to soil C persistence on centennial timescales, but are relevant for C cycling on shorter timescales as well.

Our results challenge the primacy of climatic controls on soil carbon persistence, insofar as we observed the most depleted $\Delta^{14}C_{bulk}$ in soils of the cool climate zone, not the cold climate zone. However, we found that as a categorical predictor, climate is critical for explaining the dynamics of both persistent and more transient soil C pools (as measured by proxy with $\Delta^{14}C_{bulk}$ and $\Delta^{14}C_{respired}$, respectively). Interestingly, our results indicate that soil mineral characteristics moderate the strength of the climate effect. This is particularly apparent at depth. These findings are supported by a recent study in which the authors used a depth-resolved model with energy and substrate limitation prescribed by Michalis Menten kinetics to model profiles of $\Delta^{14}C_{bulk}$ (Ahrens et al., 2020). The authors found that MAT could only explain a minimal amount of variation in the observed radiocarbon profiles, while varying sorption potential in the model allowed for a superior fit.

Previous work at our study sites showed that PCMs were key to explaining both soil C accumulation and $\Delta^{14}C_{bulk}$ values in these soils (Rasmussen et al., 2018b). Our results confirm these findings and extend them to demonstrate a highly significant correlation between PCM abundance and $\Delta^{14}C_{respired\text{-}bulk}$ ($\alpha = 0.001$), and a significant correlation with $\Delta^{14}C_{respired}$ ($\alpha = 0.1$). We focus here on $\Delta^{14}C_{respired\text{-}bulk}$, as this metric offers a unique insight into the magnitude of the difference between the cycling rates of persistent and more transiently cycling soil C.

We would expect the greatest differences between $\Delta^{14}C_{respired}$ and $\Delta^{14}C_{bulk}$ to be found in soils with a pool of old soil C protected from decomposition, and another pool of soil C that is readily decomposed. In contrast, the smallest differences should occur in soils lacking strong soil C protection mechanisms, in which the majority of soil C has an equal probability of being decomposed by microbes. Accordingly, we observed the smallest differences between $\Delta^{14}C_{respired}$ and $\Delta^{14}C_{bulk}$ in the soils with the lowest abundance of PCMs, while we observed the largest differences in the soils with the highest concentrations of these minerals (Fig. 5). We interpret these findings as evidence for a key role of PCMs in protecting soil organic matter from decomposition. The values of $\Delta^{14}C_{bulk}$ in the subsurface layers (0.1–0.3 m) of the soils lacking substantial concentration of PCMs (e.g. granitic soils) were depleted relative to the atmosphere, which indicates the presence of persistent soil C, yet we also observed similarly depleted values of $\Delta^{14}C_{respired}$ in these soils. Given that respiration rates were of the same magnitude across all soils (SI Fig. 2), this suggests that soil C persistence in these soils is due to physical constraints on decomposition that are alleviated under laboratory incubation conditions, for example transport or isolation (Gleixner, 2013).

The soils with the greatest differences between $\Delta^{14}C_{respired}$ and $\Delta^{14}C_{bulk}$ were those that had both strongly depleted values of $\Delta^{14}C_{bulk}$ and values of $\Delta^{14}C_{respired}$ that were enriched relative to the atmosphere. If we employ a theoretical compartmental model to interpret this finding, a possible scenario would involve one pool of centennial to millennially cycling soil C whose signal dominates the $\Delta^{14}C_{bulk}$ signal, and second pool of soil C enriched with C fixed from the atmosphere in the years immediately following the bomb-C spike, e.g. 1964 to 1990, whose signal dominates the $\Delta^{14}C_{respired}$ signal. More complex model structures could potentially be fit to these data, but the data provide clear evidence for the presence of at least two distinct pools: one with strongly depleted C largely inaccessible to the microbial community, and another pool enriched with

decadally cycling C that is preferentially respired. This scenario can be contrasted to the soils with $\Delta^{14}C_{respired}$ values close to that of the atmosphere, in which the respired signal is likely dominated by close to annually cycling C.

Laboratory studies on soil organic matter associations with PCMs such as goethite show that only a portion of the organic matter is so tightly bound as to resist desorption (Kaiser and Guggenberger, 2003). Further studies have demonstrated that a portion of the organic matter can be mobilized by exchange with dissolved organic C (DOC) (Leinemann et al., 2018; Liebmann et al., 2022). In this scenario, the highly depleted $\Delta^{14}C_{bulk}$ values observed in the soils with a high abundance of PCMs may derive from organic matter that is strongly sorbed to mineral surfaces or trapped in micropores, while the bomb-C enriched decadally cycling C observed in the respiration flux could derive from a more microbially accessible and DOC-exchangeable mineral associated soil C pool that is in someway facilitated by PCMs (e.g. organo-metal complexes, cf. Lawrence et al., 2015; Heckman et al., 2018). However, the rates of change over time that we observed for $\Delta^{14}C_{respired}$ indicate that annually cycling C is also an important component of soil organic matter at all of our sites.

Our finding that parent material explains more of the variation in $\Delta^{14}C_{respired}$ at depth than climate suggests that, in deeper soil layers, the role of soil minerals in regulating annually to decadally cycling soil C is of particular importance. DOC has been shown to move downward through the soil profile via preferential sorption of new soil C inputs and corresponding desorption of older DOC, which is then available to the microbial community (Kaiser and Kalbitz, 2012). This process is mineral controlled, and while we did not test it directly, such a process could explain why we see an increase in the importance of parent material, and the interaction between climate and parent material, for explaining $\Delta^{14}C_{respired}$ trends with depth.

In contrast to what we observed for PCMs, the lack of correlation we observed between CRMs and soil radiocarbon suggests that these minerals do not play an important role in explaining soil C persistence, at least in these soils. Other studies have shown that crystalline Fe oxides do protect soil C from microbial decomposition, but that the overall sorption capacity of these mineral species is low (Kahle et al., 2003). We observed a large increase in the amount of iron dissolved from CRMs at the warm sites relative to the cool or cold sites, coinciding with a decrease in soil C concentration, and relative enrichment in both $\Delta^{14}C_{bulk}$ and $\Delta^{14}C_{respired}$. The increase in CRM abundance was also associated with a corresponding decrease in PCMs. Together these trends suggest that these soils have lost PCMs through leaching and transformation into CRM species. Taken together, the patterns of C concentrations, associated SOC stocks, $\Delta^{14}C_{bulk}$, and $\Delta^{14}C_{respired}$ observed across the climate/weathering gradient suggest that weathering and crystallization of PCMs leads to a reduction in soil carbon stocks caused by losses of old $\Delta^{14}C$-depleted carbon associated with these minerals, and that this process is relevant across a range of igneous parent materials.

The sensitivity of decomposition to temperature is of particular interest for understanding how soil C dynamics may change under a warming climate. Comparing the change in $\Delta^{14}C_{respired}$ over time for the different climate zones across the different

lithologies provides insight into this question. Focusing on the near surface soils (0–0.1 m), where climate effects are strongest, we observed that the rate of change in $\Delta^{14}C_{respired}$ over time was correlated with PCM abundance. We observed a linear relationship between MAT and the rate of change in $\Delta^{14}C_{respired}$ over time for the granitic soils, which had low abundances of PCMs in all three climate zones. This relationship was absent for the basalt and andesitic soils, which had higher concentrations of PCMs in the cool climate zone than in the cold climate zone. Furthermore, the change in $\Delta^{14}C_{respired}$ over time was similar in all of the warm climate zone soils lacking substantial PCM content. These findings provide evidence that the presence of PCMs is associated with a decoupling of MAT and soil C cycling rates, which suggests that PCMs may attenuate the temperature sensitivity of soil organic matter decomposition. If this is true, we would expect that potential increases in decomposition rates, and accompanying carbon losses due to climate warming, would be greater in soils lacking PCMs than in soils enriched in these mineral species.

5 Conclusion

Our study shows clearly that parent material and climate interact to control soil C dynamics. This interaction is the key to explain trends in $\Delta^{14}C_{bulk}$, which is a proxy for the mean age of soil C, and additionally in $\Delta^{14}C_{respired}$, which reveals the relative contributions of faster or more slowly cycling soil C to respiration. We were unable to explain the trends in $\Delta^{14}C_{bulk}$, or $\Delta^{14}C_{respired}$ across all sites with MAT, demonstrating the limits of relying on the temperature-decomposition relationship in determining soil C persistence, and the importance of considering soil mineral assemblages.

The results of this study imply that parent material and soil development rates can be equal in importance to temperature when determining soil C persistence. Specifically, intermediate aged soils developed on parent materials with the potential for substantial PCM development, such as basalt or andesite, can be expected to accumulate more C than soils lacking this potential, such as granite. Furthermore, changes in environmental conditions that accelerate the loss of PCMs via leaching or crystallization, e.g. low redox potential, low pH, warm temperatures and adequate moisture, can be expected to lead to SOC stock losses and a lower capacity to store soil C once the system returns to steady-state. Finally, the signal from decadally cycling soil C in $\Delta^{14}C_{respired}$ observed at the sites most enriched with PCMs provides preliminary evidence that the association of soil organic matter with these mineral phases may attenuate the temperature sensitivity of decomposition.

Code/Data availability

All data and code required to reproduce the analyses are available on Zenodo (Beem-Miller, 2022).

Author contributions

JBM and CR conceptualized this study, collected samples, and conducted laboratory analyses. JBM conducted data analysis. ST provided funding and radiocarbon expertise. All authors contributed to the discussion of results and manuscript preparation.

Competing interest

The authors declare that they have no conflict of interests.

Acknowledgements

C. Rasmussen for the initiating the sites, sharing archived data, and field assistance; M. Rost for laboratory assistance; S. von Fromm for field assistance; A. Steinhof and the Jena AMS team for assisting with radiocarbon analyses.

Financial support

This work was supported with funding from the European Research Council (Horizon, 2020 Research and Innovation Programme, grant agreement 695101; 14Constraint). Open access funding enabled and organized by Projekt DEAL.

References

Abramoff, R. Z., Torn, M. S., Georgiou, K., Tang, J., and Riley, W. J.: Soil Organic Matter Temperature Sensitivity Cannot be Directly Inferred From Spatial Gradients, Global Biogeochemical Cycles, 33, 761–776, https://doi.org/10.1029/2018GB006001, 2019.

Ahrens, B., Guggenberger, G., Rethemeyer, J., John, S., Marschner, B., Heinze, S., Angst, G., Mueller, C. W., Kögel-Knabner, I., Leuschner, C., Hertel, D., Bachmann, J., Reichstein, M., and Schrumpf, M.: Combination of energy limitation and sorption capacity explains 14C depth gradients, Soil Biology and Biochemistry, 148, https://doi.org/10.1016/j.soilbio.2020.107912, 2020.

Baisden, W. T., Amundson, R., Cook, A. C., and Brenner, D. L.: Turnover and storage of C and N in five density fractions from California annual grassland surface soils, Global Biogeochemical Cycles, 16, 64-1-64–16, https://doi.org/10.1029/2001gb001822, 2002.

Baisden, W. T., Parfitt, R. L., Ross, C., Schipper, L. A., and Canessa, S.: Evaluating 50 years of time-series soil radiocarbon data : towards routine calculation of robust C residence times, Biogeochemistry, 112, 129–137, https://doi.org/10.1007/s10533-011-9675-y, 2013.

Beem-Miller, J.: v1.0 jb388/sra-ts: Submission to SOIL (Copernicus) 11 Oct 2022, 2022. https://doi.org/10.5281/zenodo.7186755

Beem-Miller, J., Schrumpf, M., Hoyt, A. M., Guggenberger, G., and Trumbore, S.: Impacts of Drying and Rewetting on the Radiocarbon Signature of Respired CO2 and Implications for Incubating Archived Soils, Journal of Geophysical Research: Biogeosciences, 126, 1–17, https://doi.org/10.1029/2020JG006119, 2021.

Beem-Miller, J. P., Kong, A. Y. Y., Ogle, S., and Wolfe, D.: Sampling for soil carbon stock assessment in rocky agricultural soils, Soil Science Society of America Journal, 80, https://doi.org/10.2136/sssaj2015.11.0405, 2016.

Bishop, T. F. a, McBratney, a. B., and Laslett, G. M.: Modeling soil attribute depth functions with equal-area quadratic smoothing splines, Geoderma, 91, 27–45, https://doi.org/10.1016/S0016-7061(99)00003-8, 1999.

Castanha, C., Trumbore, S., and Amundson, R.: Methods of separating soil carbon pools affect the chemistry and turnover time of isolated fractions, Radiocarbon, 50, 83–97, https://doi.org/10.1017/S0033822200043381, 2008.

Crow, S. E. and Sierra, C. A.: The climate benefit of sequestration in soils for warming mitigation, Biogeochemistry, https://doi.org/10.1007/s10533-022-00981-1, 2022.

Dahlgren, R. A., Boettinger, J. L., Huntington, G. L., and Amundson, R. G.: Soil development along an elevational transect in the western Sierra Nevada, California, Geoderma, 78, 207–236, https://doi.org/10.1016/S0016-7061(97)00034-7, 1997.

Davidson, E. A. and Janssens, I. A.: Temperature sensitivity of soil carbon decomposition and feedbacks to climate change, Nature, 440, 165–173, https://doi.org/10.1038/nature04514, 2006.

Davidson, E. A., Trumbore, S. E., and Amundson, R.: Soil warming and organic carbon content, Nature, 408, 789–790, https://doi.org/10.1038/35048672, 2000.

Duiker, S. W., Rhoton, F. E., Torrent, J., Smeck, N. E., and Lal, R.: Iron (Hydr)Oxide Crystallinity Effects on Soil Aggregation, Soil Science Society of America Journal, 67, 606–611, https://doi.org/10.2136/sssaj2003.6060, 2003.

Ewing, S. A., Sanderman, J., Baisden, W. T., Wang, Y., and Amundson, R.: Role of large-scale soil structure in organic carbon turnover: Evidence from California grassland soils, Journal of Geophysical Research: Biogeosciences, 111, 1–9, https://doi.org/10.1029/2006JG000174, 2006.

Frank, D. A., Pontes, A. W., and McFarlane, K. J.: Controls on Soil Organic Carbon Stocks and Turnover Among North American Ecosystems, Ecosystems, 15, 604–615, https://doi.org/10.1007/s10021-012-9534-2, 2012.

Gleixner, G.: Soil organic matter dynamics: A biological perspective derived from the use of compound-specific isotopes studies, Ecological Research, 28, 683–695, https://doi.org/10.1007/s11284-012-1022-9, 2013.

Graham, R. C. and O'Geen, A. T.: Soil mineralogy trends in California landscapes, Geoderma, 154, 418–437, https://doi.org/10.1016/j.geoderma.2009.05.018, 2010.

Graven, H., Allison, C. E., Etheridge, D. M., Hammer, S., Keeling, R. F., Levin, I., Meijer, H. A. J., Rubino, M., Tans, P. P., Trudinger, C. M., Vaughn, B. H., and White, J. W. C.: Compiled records of carbon isotopes in atmospheric CO2 for historical simulations in CMIP6, Geoscientific Model Development, 10, 4405–4417, https://doi.org/10.5194/gmd-10-4405-2017, 2017.

Harradine, F. and Jenny, H.: Influence of parent material and climate on texture and nitrogen and carbon contents of virgin California soils: I. Texture and nitrogen contents of soils, Soil Science, 85, 235–243, https://doi.org/10.1097/00010694-195805000-00001, 1958.

Heckman, K., Lawrence, C. R., and Harden, J. W.: A sequential selective dissolution method to quantify storage and stability of organic carbon associated with Al and Fe hydroxide phases, Geoderma, 312, 24–35, https://doi.org/10.1016/j.geoderma.2017.09.043, 2018.

Hengl, T.: GSIF: Global Soil Information Facilities, 2019. https://CRAN.R-project.org/package=GSIF

Hopkins, F. M., Torn, M. S., and Trumbore, S. E.: Warming accelerates decomposition of decades-old carbon in forest soils (SI), Proceedings of the National Academy of Sciences, 1–6, https://doi.org/10.1073/pnas.1206575109, 2012.

Hua, Q., Turnbull, J. C., Santos, G. M., Rakowski, A. Z., Ancapichún, S., De Pol-Holz, R., Hammer, S., Lehman, S. J., Levin, I., Miller, J. B., Palmer, J. G., and Turney, C. S. M.: Atmospheric radiocarbon for the period 1950-2019, Radiocarbon, 64, https://doi.org/10.1017/RDC.2021.95, 2021.

Jenny, H., Gessel, S. P., and Bingham, F.T.: Comparative Study of Decomposition Rates of Organic Matter in Temperate and Tropical Regions, Soil Science, 68, 419–432, 1949.

Kahle, M., Kleber, M., and Jahn, R.: Retention of dissolved organic matter by illitic soils and clay fractions: Influence of mineral phase properties, Journal of Plant Nutrition and Soil Science, 166, 737–741, https://doi.org/10.1002/jpln.200321125, 2003.

Kahle, M., Kleber, M., and Jahn, R.: Retention of dissolved organic matter by phyllosilicate and soil clay fractions in relation to mineral properties, Organic Geochemistry, 35, 269–276, https://doi.org/10.1016/j.orggeochem.2003.11.008, 2004.

Kaiser, K. and Guggenberger, G.: Mineral surfaces and soil organic matter, European Journal of Soil Science, 54, 219–236, https://doi.org/10.1046/j.1365-2389.2003.00544.x, 2003.

Kaiser, K. and Kalbitz, K.: Cycling downwards - dissolved organic matter in soils, Soil Biology and Biochemistry, 52, 29–32, https://doi.org/10.1016/j.soilbio.2012.04.002, 2012.

Kleber, M., Mikutta, R., Torn, M. S., and Jahn, R.: Poorly crystalline mineral phases protect organic matter in acid subsoil horizons, European Journal of Soil Science, 56, 717–725, https://doi.org/10.1111/j.1365-2389.2005.00706.x, 2005.

Kleber, M., Sollins, P., and Sutton, R.: A conceptual model of organo-mineral interactions in soils: Self-assembly of organic molecular fragments into zonal structures on mineral surfaces, Biogeochemistry, 85, 9–24, https://doi.org/10.1007/s10533-007-9103-5, 2007.

Kleber, M., Eusterhues, K., Keiluweit, M., Mikutta, C., Mikutta, R., and Nico, P. S.: Mineral-Organic Associations: Formation, Properties, and Relevance in Soil Environments, Elsevier Ltd, 1–140 pp., https://doi.org/10.1016/bs.agron.2014.10.005, 2015.

Koarashi, J., Hockaday, W. C., Masiello, C. a., and Trumbore, S. E.: Dynamics of decadally cycling carbon in subsurface soils, Journal of Geophysical Research G: Biogeosciences, 117, G03033, https://doi.org/10.1029/2012JG002034, 2012.

Kramer, M. G. and Chadwick, O. A.: Controls on carbon storage and weathering in volcanic soils across a high-elevation climate gradient on Mauna Kea, Hawaii, Ecology, 97, 2384–2395, https://doi.org/10.1002/ecy.1467, 2016.

Kramer, M. G. and Chadwick, O. A.: Climate-driven thresholds in reactive mineral retention of soil carbon at the global scale, Nature Climate Change, 8, 1104–1108, https://doi.org/10.1038/s41558-018-0341-4, 2018.

Lavallee, J. M., Soong, J. L., and Cotrufo, M. F.: Conceptualizing soil organic matter into particulate and mineral-associated forms to address global change in the 21st century, Global Change Biology, 26, 261–273, https://doi.org/10.1111/gcb.14859, 2020.

Lawrence, C. R., Harden, J. W., Xu, X., Schulz, M. S., and Trumbore, S. E.: Long-term controls on soil organic carbon with depth and time: A case study from the Cowlitz River Chronosequence, WA USA, Geoderma, 247–248, 73–87, https://doi.org/10.1016/j.geoderma.2015.02.005, 2015.

Lehmann, J. and Kleber, M.: The contentious nature of soil organic matter, Nature, 528, 60–68, https://doi.org/10.1038/nature16069, 2015.

Leinemann, T., Preusser, S., Mikutta, R., Kalbitz, K., Cerli, C., Höschen, C., Mueller, C. W., Kandeler, E., and Guggenberger, G.: Multiple exchange processes on mineral surfaces control the transport of dissolved organic matter through soil profiles, Soil Biology and Biochemistry, 118, 79–90, https://doi.org/10.1016/j.soilbio.2017.12.006, 2018.

Lenth, R. V.: emmeans: Estimated Marginal Means, aka Least-Squares Means, 2021. https://CRAN.R-project.org/package=emmeans

Liebmann, P., Mikutta, R., Kalbitz, K., Wordell-Dietrich, P., Leinemann, T., Preusser, S., Mewes, O., Perrin, E., Bachmann, J., Don, A., Kandeler, E., Marschner, B., Schaarschmidt, F., and Guggenberger, G.: Biogeochemical limitations of carbon stabilization in forest subsoils, Journal of Plant Nutrition and Soil Science, 185, 35–43, https://doi.org/10.1002/jpln.202100295, 2022.

Masiello, C. A., Chadwick, O. A., Southon, J., Torn, M. S., and Harden, J. W.: Weathering controls on mechanisms of carbon storage in grassland soils C, Global Biogeochemical Cycles, 2004.

Mathieu, J. A., Hatté, C., Balesdent, J., and Parent, É.: Deep soil carbon dynamics are driven more by soil type than by climate: a worldwide meta-analysis of radiocarbon profiles, Global Change Biology, n/a-n/a, https://doi.org/10.1111/gcb.13012, 2015.

Mikutta, R., Kaiser, K., Dörr, N., Vollmer, A., Chadwick, O. A., Chorover, J., Kramer, M. G., and Guggenberger, G.: Mineralogical impact on organic nitrogen across a long-term soil chronosequence (0.3-4100 kyr), Geochimica et Cosmochimica Acta, 74, 2142–2164, https://doi.org/10.1016/j.gca.2010.01.006, 2010.

Parker, I. and Matyas, W. J.: CALVEG: A Classification of Californian Vegetation, U.S. Dep. Agric., For. Serv., Reg. Ecol. Group, San Francisco, CA, USA, 1981.

Rasmussen, C.: Pedogenesis, Soil Mineralogy, and Soil Carbon Dynamics in Sierra Nevada Conifer Systems of California, 246, 2004.

Rasmussen, C., Torn, M. S., and Southard, R. J.: Mineral Assemblage and Aggregates Control Carbon Dynamics in a California Conifer Forest, Soil Science Society of America Journal, 69, 1711–1721, https://doi.org/10.2136/sssaj2005.0040, 2005.

Rasmussen, C., Southard, R. J., and Horwath, W. R.: Soil Mineralogy Affects Conifer Forest Soil Carbon Source Utilization and Microbial Priming, Soil Science Society of America Journal, 71, 1141, https://doi.org/10.2136/sssaj2006.0375, 2007.

Rasmussen, C., Dahlgren, R. A., and Southard, R. J.: Basalt weathering and pedogenesis across an environmental gradient in the southern Cascade Range, California, USA, Geoderma, 154, 473–485, https://doi.org/10.1016/j.geoderma.2009.05.019, 2010a.

Rasmussen, C., Matsuyama, N., Dahlgren, R. A., Southard, R. J., and Brauer, N.: Soil Genesis and Mineral Transformation Across an Environmental Gradient on Andesitic Lahar, Soil Science Society of America Journal, 71, 225, https://doi.org/10.2136/sssaj2006.0100, 2010b.

Rasmussen, C., Heckman, K., Wieder, W. R., Keiluweit, M., Lawrence, C. R., Berhe, A. A., Blankinship, J. C., Crow, S. E., Druhan, J. L., Hicks Pries, C. E., Marin-Spiotta, E., Plante, A. F., Schädel, C., Schimel, J. P., Sierra, C. A., Thompson, A., and Wagai, R.: Beyond clay: towards an improved set of variables for predicting soil organic matter content, Biogeochemistry, 137, 297–306, https://doi.org/10.1007/s10533-018-0424-3, 2018a.

Rasmussen, C., Throckmorton, H., Liles, G., Heckman, K., Meding, S., and Horwath, W. R.: Controls on Soil Organic Carbon Partitioning and Stabilization in the California Sierra Nevada, Soil Systems, 2018b.

Schrumpf, M., Kaiser, K., Guggenberger, G., Persson, T., Kögel-Knabner, I., and Schulze, E. D.: Storage and stability of organic carbon in soils as related to depth, occlusion within aggregates, and attachment to minerals, Biogeosciences, 10, 1675–1691, https://doi.org/10.5194/bg-10-1675-2013, 2013.

Shi, Z., Allison, S. D., He, Y., Levine, P. A., Hoyt, A. M., Beem-Miller, J., Zhu, Q., Wieder, W. R., Trumbore, S., and Randerson, J. T.: The age distribution of global soil carbon inferred from radiocarbon measurements, Nature Geoscience, 13, 555–559, https://doi.org/10.1038/s41561-020-0596-z, 2020.

Sierra, C. A.: Forecasting atmospheric radiocarbon decline to pre-bomb values, Radiocarbon, 60, 1055–1066, https://doi.org/10.1017/RDC.2018.33, 2018.

Sierra, C. A., Müller, M., Metzler, H., Manzoni, S., and Trumbore, S. E.: The muddle of ages, turnover, transit, and residence times in the carbon cycle, Global Change Biology, 23, 1763–1773, https://doi.org/10.1111/gcb.13556, 2017.

Sierra, C. A., Hoyt, A. M., He, Y., and Trumbore, S. E.: Soil Organic Matter Persistence as a Stochastic Process: Age and Transit Time Distributions of Carbon in Soils, Global Biogeochemical Cycles, 32, 1574–1588, https://doi.org/10.1029/2018GB005950, 2018.

Slessarev, E. W., Chadwick, O. A., Sokol, N. W., Nuccio, E. E., and Pett-Ridge, J.: Rock weathering controls the potential for soil carbon storage at a continental scale, Biogeochemistry, 157, 1–13, https://doi.org/10.1007/s10533-021-00859-8, 2022.

Steinhof, A., Altenburg, M., and Machts, H.: Sample Preparation at the Jena 14C Laboratory, Radiocarbon, 59, 815–830, https://doi.org/10.1017/RDC.2017.50, 2017.

Stoner, S. W., Hoyt, A. M., Trumbore, S., Sierra, C. A., Schrumpf, M., Doetterl, S., Baisden, W. T., and Schipper, L. A.: Soil organic matter turnover rates increase to match increased inputs in grazed grasslands, Biogeochemistry, 156, 145–160, https://doi.org/10.1007/s10533-021-00838-z, 2021.

Stuiver, M. and Polach, H. A.: Reporting of 14C Data, Radiocarbon, 19, 355–363, https://doi.org/10.1017/S0033822200003672, 1977.

Tang, J. and Riley, W. J.: Weaker soil carbon–climate feedbacks resulting from microbial and abiotic interactions, Nature Clim Change, 5, 56–60, https://doi.org/10.1038/nclimate2438, 2014.

Tang, J. and Riley, W. J.: Competitor and substrate sizes and diffusion together define enzymatic depolymerization and microbial substrate uptake rates, Soil Biology and Biochemistry, 139, 107624, https://doi.org/10.1016/j.soilbio.2019.107624, 2019.

Torn, M. S., Trumbore, S. E., Chadwick, O. A., Vitousek, P. M., and Hendricks, D. M.: Mineral control of soil organic carbon storage and turnover, Nature, 389, 170–173, 1997.

Trumbore, S.: Age of soil organic matter and soil respiration: Radiocarbon constraints on belowground C dynamics, Ecological Applications, 10, 399–411, https://doi.org/10.1890/1051-0761(2000)010[0399:AOSOMA]2.0.CO;2, 2000.

Trumbore, S.: Radiocarbon and Soil Carbon Dynamics, Annual Review of Earth and Planetary Sciences, 37, 47–66, https://doi.org/10.1146/annurev.earth.36.031207.124300, 2009.

Trumbore, S. E., Chadwick, O. A., and Amundson, R.: Rapid Exchange between Soil Carbon and Atmospheric Carbon Dioxide Driven by Temperature Change, Science, 272, 393–396, 1996.

Woolf, D. and Lehmann, J.: Microbial models with minimal mineral protection can explain long-term soil organic carbon persistence, Scientific Reports, 9, 1–8, https://doi.org/10.1038/s41598-019-43026-8, 2019.